Structure–function analysis of HKE4, a member of the new LIV-1 subfamily of zinc transporters

Kathryn M. TAYLOR[1], Helen E. MORGAN, Andrea JOHNSON and Robert I. NICHOLSON

Tenovus Cancer Research Centre, Welsh School of Pharmacy, Cardiff University, Redwood Building, King Edward VII Avenue, Cardiff CF10 3XF, U.K.

The KE4 proteins are an emerging group of proteins with little known functional data. In the present study, we report the first characterization of the recombinant human KE4 protein in mammalian cells. The KE4 sequences are included in the subfamily of ZIP (Zrt-, Irt-like Proteins) zinc transporters, which we have termed LZT (**L**IV-1 subfamily of **Z**IP zinc **T**ransporters). All these LZT sequences contain similarities to ZIP transporters, including the consensus sequence in transmembrane domain IV, which is essential for zinc transport. However, the new LZT subfamily can be separated from other ZIP transporters by the presence of a highly conserved potential metalloprotease motif (HEXPHEXGD) in transmembrane domain V. Here we report the location of HKE4 on intracellular membranes, including the endoplasmic reticulum, and its ability to increase the intracellular free zinc as measured with the zinc-specific fluorescent dye, Newport Green, in a time-, temperature- and concentration-dependent manner. This is in contrast with the zinc influx ability of another LZT protein, LIV-1, which was due to its plasma membrane location. Therefore we have added to the functionality of LZT proteins by reporting their ability to increase intracellular-free zinc, whether they are located on the plasma membrane or on intracellular membranes. This result, in combination with the crucial role that zinc plays in cell growth, emphasizes the importance of this new LZT subfamily, including the KE4 sequences, in the control of intracellular zinc homoeostasis, aberrations of which can lead to diseases such as cancer, immunological disorders and neurological dysfunction.

Key words: HKE4, LIV-1, metalloprotease, zinc transporter, ZIP transporter; SLC39A7.

INTRODUCTION

The HKE4 protein sequence is the human homologue of the mouse KE4 gene, which has been mapped to the H2-K region of the mouse major histocompatability complex [1]. The human HKE4 has been similarly mapped to the centromeric side of the HLA class II region of the genome [2–5]. Many non-HLA genes have now been identified in the HLA region.

HKE4 was originally compared with the mouse KE4 sequence, both of which contain histidine-rich charge clusters [2]. Two years later, HKE4 and mouse KE4 sequences were aligned with ZIP (Zrt-, Irt-like Proteins) transporters as unknown open reading frame sequences and shown to exhibit similarity to the consensus sequence for ZIP transporters in TM (transmembrane) domain IV [6]. However, despite this obvious resemblance, it was evident that TM V did not share the same degree of similarity to these ZIP transporters [6,7]. When HKE4 was aligned with the oestrogen-regulated gene, LIV-1, it was clear that the sequence similarity extended across both TM IV and V [8] and was contained within 39 other sequences from over 12 species [9]. The highly conserved motif of 66 amino acids, including a novel metalloprotease motif (HEXPHEXGD), was recognized as the signature sequence of this group of proteins named as the LZT (**L**IV-1 subfamily of **Z**IP zinc **T**ransporters) subfamily of ZIP transporters [9]. Interestingly, this motif is not present in the sequences of the other three subfamilies of ZIP transporters, namely ZIP subfamilies I and II and the Gufa subfamily [10]. ZIP transporters are members of the solute carrier family 39A, with HKE4 known as SLC39A7 and LIV-1 known as SLC39A6. Of the 39 LZT sequences, we have divided 16 into a KE4 subgroup [9], only two of which are human, HKE4 and LZT-Hs9.

There is little functional data available for KE4 proteins. One KE4 sequence, CATSUP (catecholamines up), a *Drosophila* gene, has been proposed to down-regulate tyrosine hydroxylase, a rate-limiting enzyme for production of dopamine in the brain [11]. This work involved the production of knockouts in *Drosophila*, which were lethal, and testing mutated partial loss of function alleles. Another KE4 sequence, the *Arabidopsis* KE4 gene, IAR1, has been suggested to transport zinc or other metals out of the ER (endoplasmic reticulum) into the cytoplasm [7].

Zinc is essential for cell growth and is a cofactor for more than 300 enzymes, representing over 50 different enzyme classes [12]. Zinc is involved in protein, nucleic acid, carbohydrate and lipid metabolism, as well as in the control of gene transcription, growth, development and differentiation [13]. Not only can zinc deficiency be detrimental, causing stunted growth and serious metabolic disorders [14], but excess can also be toxic to cells [15]. Zinc cannot passively diffuse across cell membranes; therefore, specific zinc transporter proteins are required to transport zinc into the cytosol, both from the extracellular environment and storage compartments. Therefore zinc transporter proteins have a crucial role in maintaining the cellular balance between apoptosis and cell growth, aberrations of which could lead to diseases such as cancer, immunological disorders and neurological dysfunction.

The similarity of the KE4 sequences to the other ZIP transporters, known to have a role in zinc influx, suggests a common functional role. Previous studies in mammalian cells have indicated that both hZIP1 and hZIP2 are time-, temperature- and concentration-dependent zinc uptake transporters [16,17]. Although we have described recently the ability of a member of the LZT family, LIV-1, to act as a zinc influx transporter [9,18], the role of the human KE4 sequences has not been demonstrated.

Abbreviations used: CHO, Chinese-hamster ovary; ER, endoplasmic reticulum; ZIP, Zrt-, Irt-like Proteins; LZT, **L**IV-1 subfamily of **Z**IP zinc **T**ransporters; PNGase F, peptide *N*-glycosidase F; TM, transmembrane; TPEN, *N*,*N*,*N*′,*N*′-tetrakis-(2-pyridylmethyl)ethylenediamine.

[1] To whom correspondence should be addressed (e-mail Taylorkm@cardiff.ac.uk).

Clearly, it is important to determine the role of each different subgroup of ZIP transporters in cellular zinc transport and how they co-operate in the management of cellular zinc homoeostasis in order to understand their role in normal and disease processes.

This is the first study of a human KE4 protein in mammalian cells, and here we investigate the expression of recombinant HKE4 protein. We have engineered both wild-type and TM deletion mutants to examine location, glycosylation, abundance, membrane topology and zinc transport ability. We have demonstrated the localization of HKE4 to intracellular membranes, including the ER, which is in contrast with the plasma membrane location of most of the other LZT family members such as LIV-1 [9,18]. We also show how the presence of recombinant HKE4 increases the concentration of intracellular-free zinc, confirming its role as a zinc transporter.

EXPERIMENTAL

HKE4 expression in human tissues

A commercially produced Multiple Tissue Expression array (MTE™, ClonTech), containing poly r(A) from 68 normal human tissues and eight cancer cell lines, was hybridized with a 478 bp HKE4-specific probe (65–553 bp) according to the manufacturer's instructions.

Computer prediction of the HKE4 sequence

The computer prediction of HKE4 secondary structure was achieved using the GCG [Wisconsin Package Version 9.0; Genetics Computer Group, Madison, WI, U.S.A.] package of software and others, as described previously [18]. Computer alignments of KE4 and LZT sequences were performed using CLUSTAL V [19].

Engineering HKE4 cDNA

A PCR construct of HKE4 was generated using oligonucleotide primers (overlap with HKE4 is underlined): 5′-ACAATGGCCAGAGGCCTGG-3′ and 5′-CTCAAGGTGGGCAATCAGCAC-3′ to PCR-amplify clone 1033B10 from library RPCI5 (a gift from The Sanger Centre, Cambridge, U.K.) using Biotaq DNA polymerase from Bioline (London, U.K.). The PCR product was ligated with the TOPO-TA cloning vector (Invitrogen, Paisley, U.K.), pcDNA3.1/V5-His-TOPO and cloned as described previously [18]. Constructs were validated by the BigDye Terminator cycle sequencing ready reaction kit (Applied Biosystems, Warrington, Cheshire, U.K.) and an ABI Prism 377 DNA sequencer (Applied Biosystems). TM deletion mutants of HKE4 were constructed using the same method and the following 3′-oligonucleotide primers: 5′-CCCATCTTGCAATGGTGATGCCTC-3′ to produce a 7 TM domain protein (1–449 residues), 5′-CCCATCTTTGGGTACTGTGCTCCC-3′ to produce a 3 TM domain protein (1–301 residues) and 5′-CCCATCCCGGGGAGAGTTCGA-3′ to produce a 1 TM domain protein (1–170 residues). A LIV-1 construct was engineered using the same method as described previously [18].

Expression of recombinant proteins in CHO (Chinese-hamster ovary) cells

CHO cells were maintained in minimal essential medium, α-modification (Sigma) with 10 % (v/v) foetal calf serum, 4 mM glutamine, 20 μg/ml penicillin and streptomycin and 2.5 μg/ml fungizone under 5 % CO_2 at 37 °C. Cells were transfected with the relevant pcDNA3.1/V5-His-TOPO constructs using LIPOFECTAMINE™ 2000 (Invitrogen), according to the manufacturer's instructions. Briefly, 9×10^5 cells, grown on 60 mm dishes for 24 h, were transfected with 8.8 μg of DNA and 27.5 μl of reagent in antibiotic-free media.

SDS/PAGE and Western-blot analysis

Transfected CHO cells were harvested exactly 24 h after transfection, lysed and prepared for Western blotting as described previously [18]. Control samples were either CHO cells transfected with the LacZ gene (Invitrogen) or CHO cells transfected with no DNA. Membranes were probed with anti-V5 antibody (1/5000 in 1 % non-fat milk/PBS) and visualized by chemiluminescence using West Femto reagent (PerbioScience, Cheshire, U.K.). To investigate deglycosylation, CHO cell lysate fractions expressing recombinant HKE4 and LIV-1 (as a positive control) proteins were incubated with 2 units of endoglycosidase PNGase F (peptide *N*-glycosidase F; Boehringer Ingelheim, Bracknell, U.K.) overnight at 37 °C before Western-blot analysis.

Fluorescence microscopy

Before transfection, 2.2×10^5 cells were grown on 0.17 mm thick coverslips for 24 h. Cells were fixed with 4 % (v/v) formaldehyde for 15 min, permeabilized with 0.4 % saponin in PBS for 15 min and kept in this buffer throughout, blocked with 10 % (v/v) normal goat serum, incubated with anti-V5 monoclonal antibody (1/1000) for 1 h at 25 °C. To determine the presence of HKE4 in the ER, the cells were also incubated with an anti-calreticulin polyclonal antibody (1/500), as a marker for the ER. The secondary antibodies, Alexa Fluor 488-conjugated anti-mouse and Alexa Fluor 594-conjugated anti-rabbit (both 1/1000; Molecular Probes, Europe BV, Leiden, The Netherlands), were incubated for 1 h and assembled on to slides using Vectorshield with 4,6-diamidino-2-phenylindole (Vector Laboratories, Peterborough, U.K.). All coverslips were viewed on a Leica RPE automatic microscope using a × 100 oil immersion lens. The fluorescent superimposed images were acquired using a multiple band pass filter set appropriate for 4,6-diamidino-2-phenylindole, fluorescein and Texas Red.

FACS analysis

For FACS analysis, CHO cells expressing the recombinant proteins were harvested carefully by pipette and resuspended into Krebs–Ringer Hepes buffer [20] and were incubated with 50 μM Newport Green diacetate (Molecular Probes) for 1 h at 37 °C. Addition of 25 μM zinc chloride or the zinc-specific chelator TPEN [*N*,*N*,*N*′,*N*′-tetrakis-(2-pyridylmethyl)ethylenediamine; Molecular Probes] was also at 37 °C. A Becton-Dickinson FACS III flow cytometer and software was used to analyse FACS results.

RESULTS

Computer prediction of HKE4 secondary structure

Computer prediction of HKE4 secondary structure suggests a protein with eight TM domains, a core size of 50 kDa and a cleaveable signal peptide between residues 29 and 30 (Figures 1 and 2A). HKE4 is predicted to have a long cytosolic N-terminus, short C-terminus and a location on the ER membrane (Table 1). The sequence has no obvious ER retention motif, such as a KDEL or a C-terminal dileucine motif, apart from ARGL (residues 2–5) in the N-terminus signal peptide, which would be expected to be cleaved after processing in the ER. However, it does contain both KKXX and KXKXX cytoplasmic-located dileucine motifs (at positions 377 and 271 respectively), which have been shown

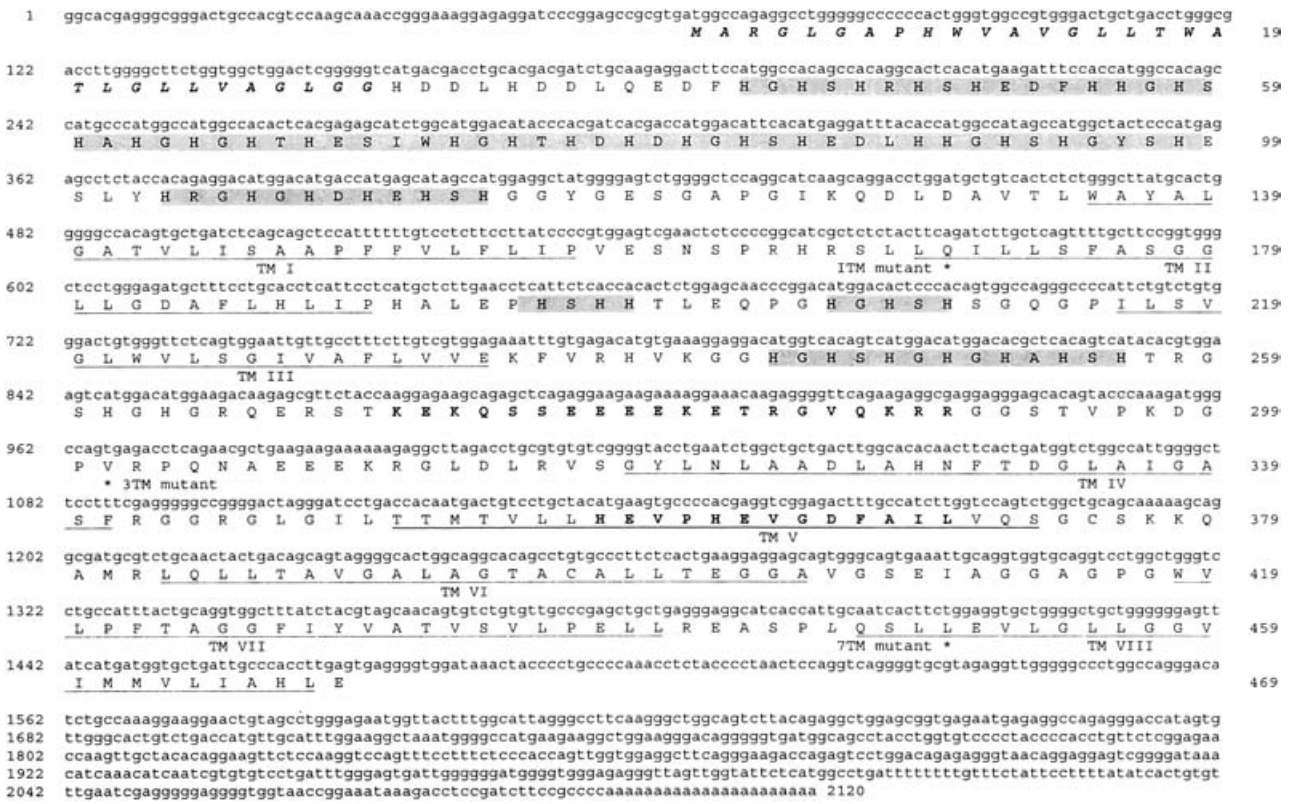

Figure 1 cDNA sequence of HKE4

cDNA sequence of HKE4 (accession no. Q9UIQ0) including the predicted amino acid sequence from the open reading frame, start position 65 bp. Potential TM domains are underlined, histidine-rich regions are shaded, signal peptide is shown in bold-italic face, catalytic zinc-binding site motif (HEXPHEXGD, residues 358–370) of the metalloprotease family and the mixed charge region (residues 271–290) are shown in boldface. The positions of the ends of the TM deletion mutants 1, 3 and 7 are indicated underneath the sequence by an asterisk. Numbers on the right refer to the amino acid sequence and numbers on the left refer to the cDNA sequence.

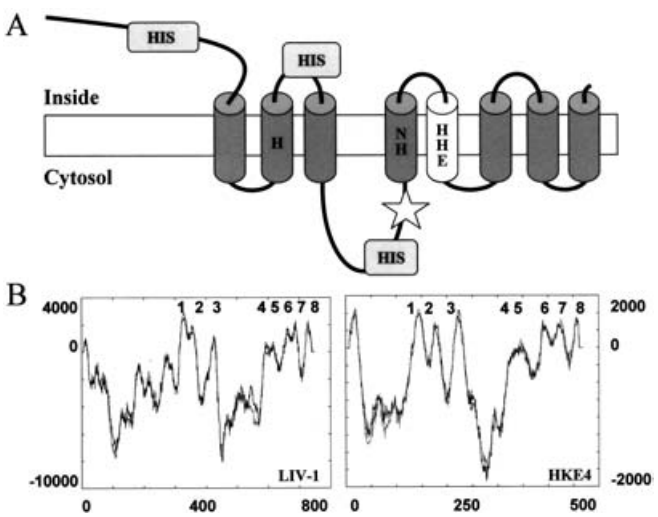

Figure 2 HKE4 secondary structure schematic and hydrophobicity plot

(**A**) N- and C-termini are predicted to be extra-cytosolic. Barrels represent TM domains, white barrel represents TM domain with conserved metalloprotease (HEX**P**H**E**) motif unique to the LZT subfamily, HIS represents (HX)*n* histidine-rich repeats, the star represents conserved mixed charge region upstream of TM IV (numbering TM domains from the left), letters in barrels represent the residues conserved in the LZT subfamily in identical or similar positions to those conserved in ZIP transporters, H in TM II, HN in TM IV and HXXHE in TM V. (**B**) Comparison of hydrophobicity plot of HKE4 and LIV-1 using TMPred [35] with numbers added to indicate predicted TM domains 1–8. Despite the longer N-terminal region of LIV-1, the hydrophobicity plot is remarkably similar to that of HKE4.

Table 1 Details of sequence motifs found in HKE4 protein sequence

HKE4 residue number	Sequence	Potential motif
2–5	ARGL	Potential ER retention signal
330	NX(S,T)	N-linked glycosylation
42–52	FHGHSHRHSHE	Histidine-rich charge runs
56–69	HGHSHAHGHGHTHE	and patterns
72–86	WHGHTHDHDHGHSHE	
105–115	GHGHDHEHSHG	
243–257	GHGHSHGHGHAHSHT	
49–60, 83–84	HSHEDFHHGHSH	Separated tandem repeats
56–64, 244–252	HGHSHAHGH	
271–290	KEKQSSEEEEKETRGVQKRR	Mixed charge region
288, 310, 289	KR, RR	Dibasic motifs as proteolysis signals [36]
238, 258, 265, 268, 281, 297, 316, 342	(R/K)X*n* (R/K) where *n* = 2, 4 or 6	Dibasic motifs recognizable by proprotein convertases [37]

to lead to ER retention of membrane proteins [21,22]. There is also a motif (HEX**P**H**E**XGD) at residues 359–367, which fits the consensus sequence for the LZT subfamily of ZIP zinc transporters [9]. This motif is predicted to be adjacent to a TM domain. However, by alignment of this area with other KE4 family members (Figure 3) and comparison of the hydrophobicity plot with that of LIV-1 (Figure 2B), it seems probable that this motif is actually within TM domain V (Figure 3), as predicted for other LZT family members. This would position the initial histidine

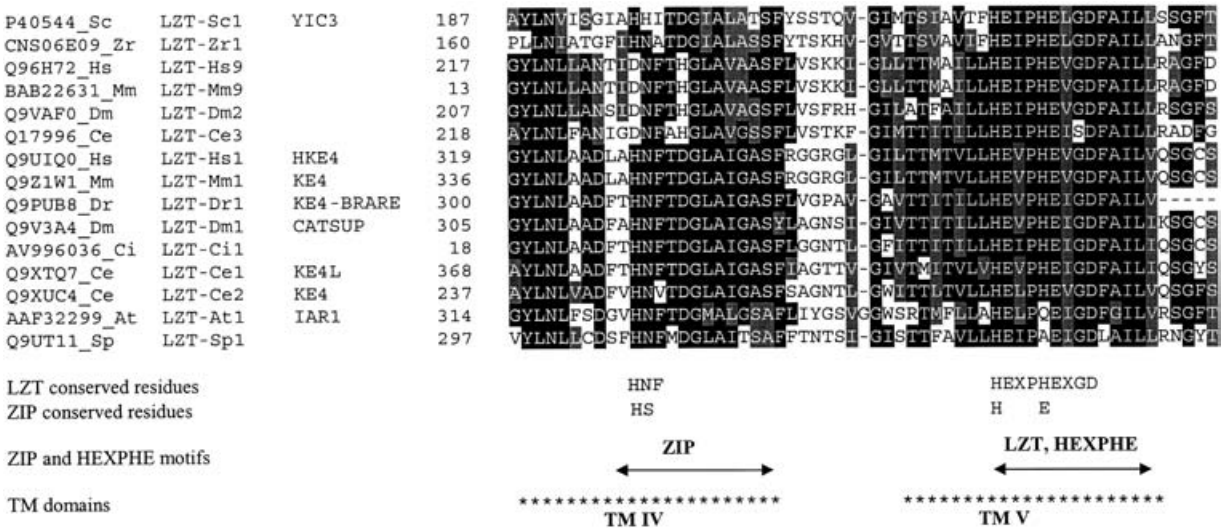

Figure 3 Alignment of the KE4 subfamily of LZT zinc transporters across TM IV and V

Residues coloured black and grey correspond to identical or complementary residues respectively. Arrows indicate the ZIP consensus sequence, including the positions of the conserved residues in ZIP transporters (HS and HXXE) and the conserved residues in the LZT subfamily (HNF and HEXPHEXGD). Accession numbers are given on the left-hand side column, followed by species indicators, LZT family name, any known gene names and residue number. It is clear that there is a high degree of conservation encompassing both motifs. Alignment of sequences was achieved in Clustal V [19].

residue of this metalloprotease motif in the same position as a conserved histidine of the ZIP transporters (Figure 3). This alignment confirms that there is a high degree of identical (black) and complementary (grey) residues shared by all KE4 sequences. Interestingly, those histidine residues that have been proven to be crucial for function in ZIP transporters (Figure 3) are also conserved in HKE4, suggesting an ability to transport zinc or other metal ions. The HKE4 sequence contains a significantly high occurrence of histidine residues [23] in the form of (HX)*n* histidine-rich repeats, where *n* is the number of repeats. Assuming both the predicted ER location of HKE4 protein and the same membrane topology as other members of the ZIP family, the histidine repeats on the N-terminus and the loop between TM II and III would be located in the ER lumen, and the histidine repeats on the loop between TM III and IV would be located in the cytosol (Figure 2A). These histidine-rich repeats contain a number of different repeated patterns (Table 1), a common feature of LZT sequences [9]. HKE4 is predicted to have an overall negative charge, which would be consistent with its expected role as a zinc transporter.

There is no strong PEST site in the HKE4 sequence, as has been observed for LIV-1, although there are some simple dibasic motifs which can target a sequence for degradative proteolysis (Table 1), including eight motifs recognized by proprotein convertases, six of which are predicted to reside in the cytosol.

The current number of LZT family sequences that contain the signature sequence HEX**PH**E**X**GD is 53, of which 21 belong to the separate KE4 subgroup (Figure 4). These LZT sequences now span 19 species in total and include mammals, insects, plants, yeast, bacteria and fungi, suggesting conservation during evolution.

Expression of recombinant HKE4 protein

We cloned the HKE4 cDNA (Q9UIQ0) into the expression vector pcDNA3.1/V5-His-TOPO to enable expression in mammalian cells from the cytomegalovirus promoter. Constructs were engineered for expression of TM deletion mutants containing in total 1, 3 or 7 TM domains to allow us to investigate the membrane topology and glycosylation. The subsequent recombinant proteins were expressed as fusion proteins with a 5 kDa V5-tag on the C-terminal end, enabling detection using the anti-V5 antibody. These plasmids were transiently transfected into CHO cells and the control CHO cells were transfected either without DNA (CHO) or with the control LacZ gene (LacZ).

To determine the mass of the recombinant HKE4 proteins, CHO cells expressing the recombinant proteins were harvested, lysed, separated by SDS/PAGE and visualized by Western-blot analysis with the anti-V5 antibody. This demonstrated a single band (56 kDa) compatible with the predicted core mass of 50 kDa for HKE4 (wild-type) and an additional 5 kDa due to the V5-tag (Figure 5A). The different mutants also produced bands compatible with their predicted masses, 55 kDa for 7 TM mutant (predicted 53 kDa), 36 kDa for 3 TM mutant (predicted 38 kDa) and 25 kDa for 1 TM mutant (predicted 24 kDa), allowing 5 kDa for the V5-tag.

Transfected cells were harvested at 24 h intervals for 5 days to determine the optimum transfection duration for maximal recombinant protein production. As the amount of protein produced was comparable between 24 and 96 h post-transfection (Figure 5B), 24 h was used for subsequent experiments.

To investigate the presence of the one predicted N-linked glycan chain at position 330 (Table 1), HKE4-transfected CHO cell lysate was treated with PNGase F to remove any such chains (Figure 5D) and compared with lysate without treatment. Because of the position of this potential site, the 3 and 1 TM mutants would not be predicted to have any glycosylated side chains. However, this treatment produced no decrease in the mass of the protein bands, indicating no glycosylation at this site. This failure to decrease the molecular mass was not due to failure of the protocol as another LZT protein (LIV-1), which did contain N-linked glycan chains, gave a 10 kDa decrease under the same conditions (Figure 5C).

Cellular location of HKE4

For HKE4 to act as a zinc influx transporter, as suggested by its similarity to ZIP transporters, it would have to reside on the plasma membrane of cells. However, the HKE4 sequence was predicted to reside in the ER (Table 1). We therefore prepared

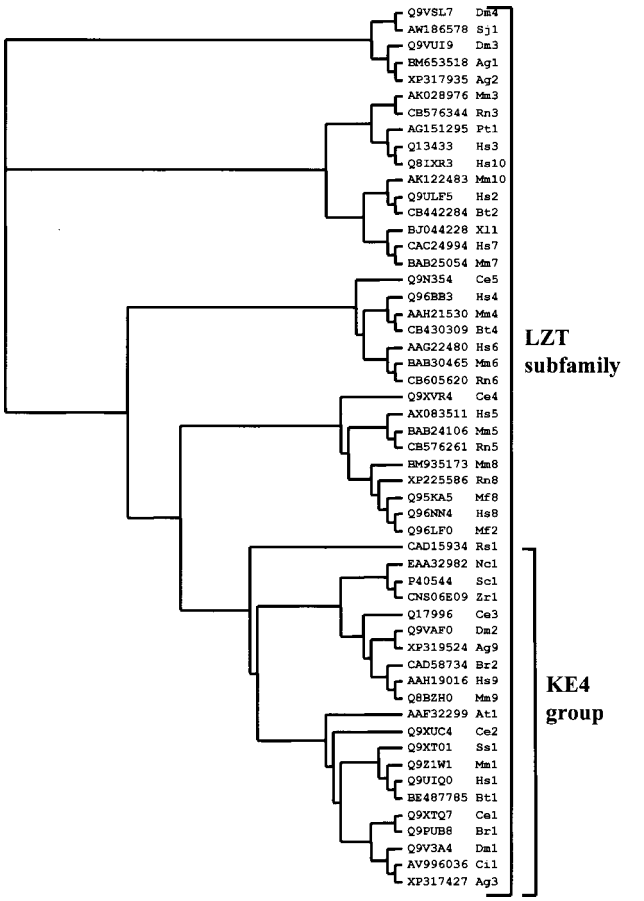

Figure 4 Phylogenetic tree of the LZT subfamily sequences

Association of 53 LZT family sequences was determined using the Clustal V [19] program to perform an alignment. This dendrogram shows how the 21 KE4 proteins form a separate section of the LIV-1 subfamily. The two-letter species abbreviations given below follow the accession number and precede the LZT family code [9]. Ag, *Anopheles gambiae*; At, *Arabidopsis thaliana*; Br, *Brachydanio rerio*; Bt, *Bos taurus*; Ce, *Caenorhabditis elegans*; Ci, *Ciona intestinalis*; Dm, *Drosophila melanogaster*; Hs, *Homo sapiens*; Mf, *Macaca fascicularis*; Mm, *Mus musculus*; Nc, *Neurospora crassa*; Pt, *Pan troglodytes*; Rn, *Rattus norvegicus*; Rs, *Ralstonia solanacearum*; Sc, *S. cerevisiae*; Sj, *Schistosoma japonicum*; Ss, *Sus scrofa*; Xl, *Xenopus laevis*; Zr, *Zygosaccharomyces rouxii*.

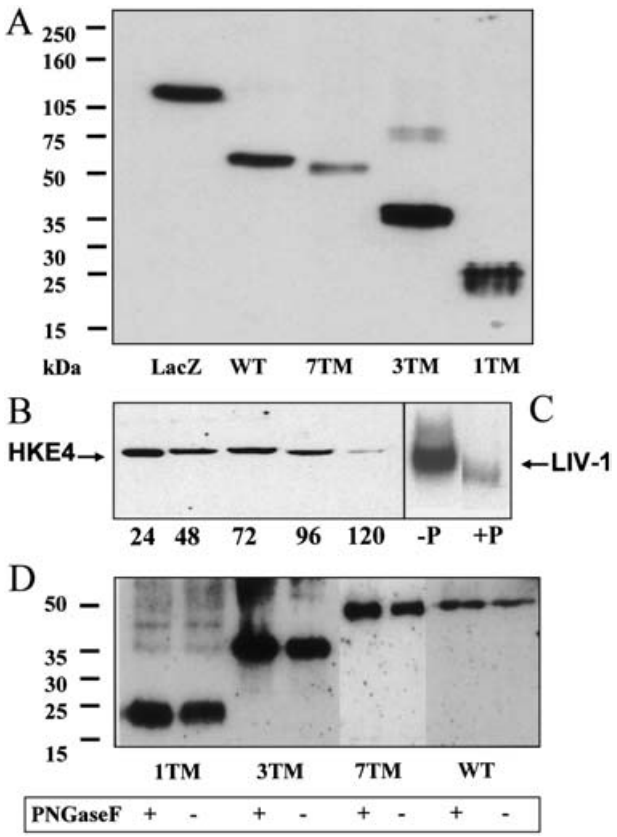

Figure 5 Western-blot analysis of recombinant HKE4 proteins

Western-blot analysis with V5 antibody of CHO cells transiently expressing HKE4 wild-type and mutant proteins. (**A**) Full-length HKE4 (WT) produces a band of approx. 56 kDa, the 7 TM mutant (7 TM) a band of 55 kDa, the 3 TM mutant (3 TM) a band of 36 kDa and the 1 TM mutant (1 TM) a band of 25 kDa. All these correspond to the predicted masses and include the 5 kDa V5 epitope. (**B**) Bands represent the amount of wild-type HKE4 produced in CHO cells at different times (in h) after transfection. (**C**) Another LZT protein, LIV-1, produced a reduction in molecular mass when incubated with PNGase F (+P) compared with without PNGase F (−P). (**D**) Incubation of CHO cell lysates expressing the wild-type (WT) and mutated HKE4 proteins (1 TM, 3 TM and 7 TM) with PNGase F produced no reduction in molecular mass, indicating no N-linked glycan chains in HKE4.

HKE4-transfected cells on coverslips for fluorescence microscopy imaging by fixing and incubating with anti-V5 antibody followed by an Alexa-488 conjugate. This imaging enabled localization of HKE4 to a structure with remarkable similarity to the network of the ER, including a perinuclear region (Figure 6A1, green). The HKE4 (Figure 6A3, red) predominantly co-localized (Figure 6A4, yellow) with an ER marker, calreticulin (Figure 6A2, green), although some resided in additional, as yet undefined, structures.

The TM deletion mutants of HKE4 located at an identical cellular region as the wild-type HKE4 (results not shown), indicated that the loss of C-terminal residues did not alter the processing. To investigate the membrane topology of the HKE4 constructs, CHO cells transfected with either the wild-type or mutant were harvested and incubated with anti-V5 antibody, followed by a fluorescent secondary antibody, before fluorescence was observed by FACS analysis. This confirmed that all the recombinant proteins were located on an intracellular membrane as no fluorescence greater than the controls was obtained from non-permeabilized cells (results not shown).

Zinc transport

To test the hypothesis that HKE4 is a functional member of the ZIP transporter family, we investigated the ability of CHO cells expressing recombinant HKE4 to alter the intracellular-free zinc content compared with control cells. Transfected cells in suspension were loaded with the cell-permeant zinc-specific fluorescent indicator Newport Green diacetate [24], which, on intracellular esterase cleavage, binds to the pool of intracellular free zinc and acts as a fluorescent indicator for intracellular labile zinc content [25,26].

The resulting basal cytosolic fluorescence of the cells was documented by FACS analysis as well as their ability to respond to changes in both extracellular and intracellular zinc concentrations. We compared the HKE4 expressing cells with those expressing LIV-1, which has been shown to act as a zinc influx transporter [18] enabled by its situation on the plasma membrane. Cells transiently expressing HKE4 had an increased resting fluorescence of $> 70\,\%$ of the CHO and LacZ control cells [Figures 6B (upper panel) and 6C]. This increase was similar to that of the LIV-1 expressing cells (Figures 6B and 6C). This result

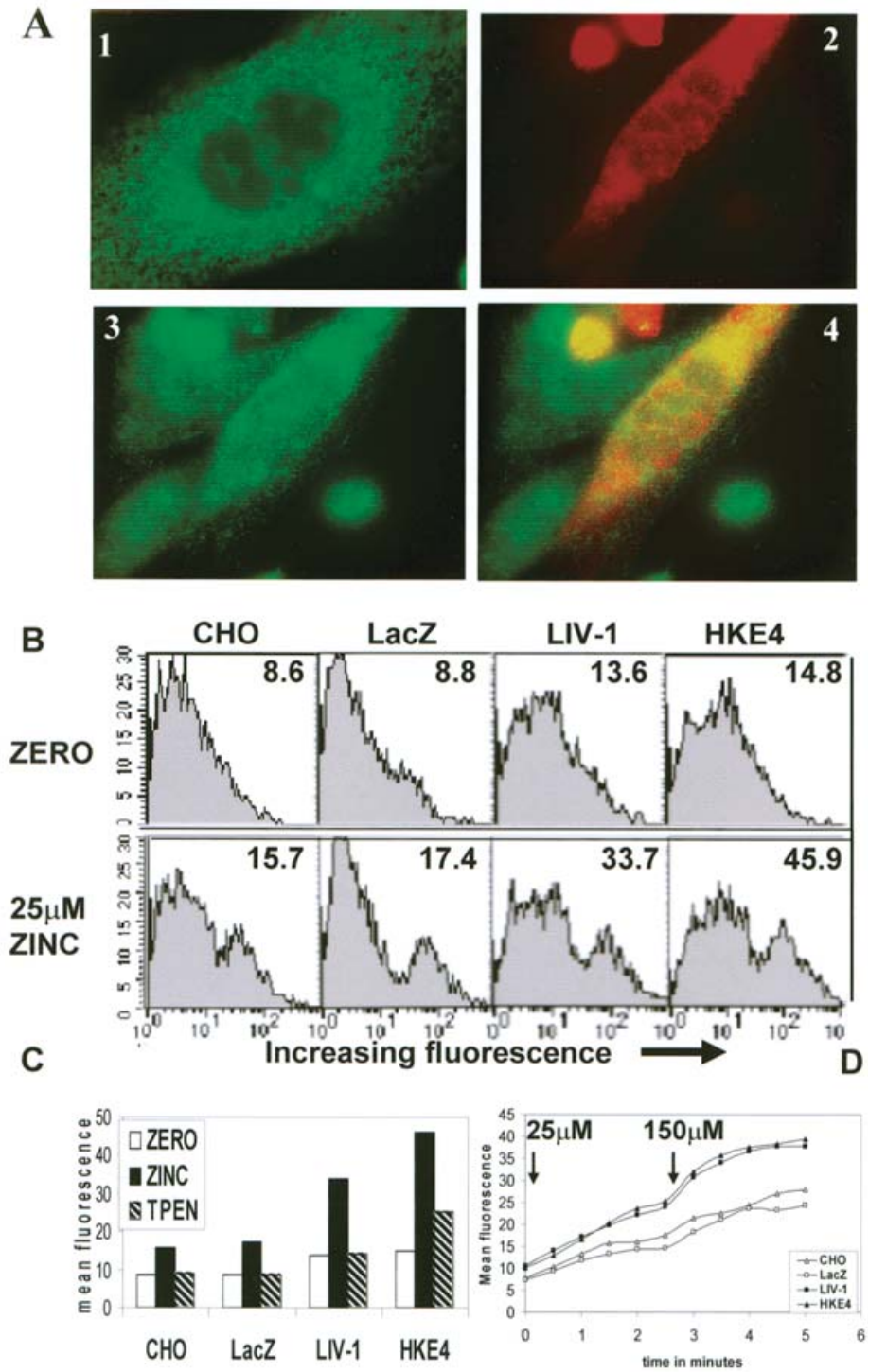

Figure 6 Imaging of recombinant HKE4 and zinc transport ability

(**A**) The HKE4-V5 fusion protein (stained green with Alexa-488) showed a typical ER network-staining pattern (panel 1) with a perinuclear band in fixed and permeabilized CHO cells. HKE4 (panel 2, stained red with Alexa-594) partially co-localizes with a calreticulin antibody (panel 3, stained green with Alexa-488) as demonstrated by the yellow colour in the overlay (panel 4). (**B**) CHO cells transiently transfected with no DNA (CHO), LIV-1 or HKE4 were loaded with Newport Green diacetate and fluorescence read by FACS under basal conditions (upper panel) or after 15 min treatment with 25 μM zinc (lower panel). Numbers in panels represent mean fluorescence values. (**C**) CHO cells expressing LIV-1 and HKE4 had increased basal fluorescence (white bars), compared with CHO and LacZ controls, which increased in all cases when incubated with 25 μM zinc for 30 min (black bars). This increase was abolished when cells were incubated further with 25 μM TPEN for 30 min, with the exception of the HKE4-expressing cells (hatched bars). (**D**) Short-term time course of zinc uptake in CHO cells expressing LIV-1 (■), HKE4 (▲), LacZ (□) or control (CHO; △) cells. Each Figure is a representative result of at least three experiments.

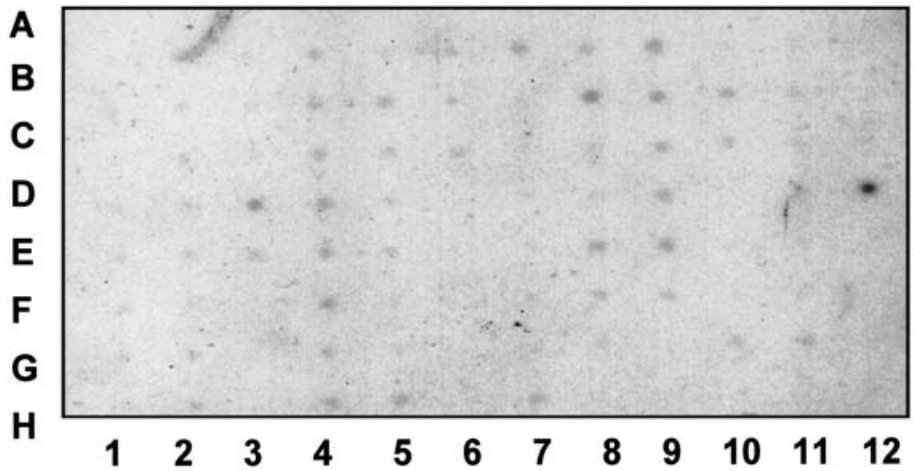

Figure 7 Expression of HKE4 in a multi-tissue array

Autoradiograph of a human multi-tissue expression array hybridized with a HKE4-specific cDNA probe. High levels of HKE4 expression are observed in placenta (B8), liver (A9), pituitary gland (D3), pancreas (B9), salivary gland (E9), kidney (A7) and prostate (E8). It can be observed that HKE4 is ubiquitously expressed in the remaining tissues, albeit at a lower level. Tissues represented on the human multi-tissue expression array: A1, whole brain; A2, left cerebellum; A3, substantia nigra; A4, heart; A5, oesophagus; A6, transverse colon; A7, kidney; A8, lung; A9, liver; A10, leukaemia HL-60; A11, foetal brain; A12, yeast total RNA; B1, cerebral cortex; B2, right cerebellum; B3, accumbens nucleus; B4, aorta; B5, stomach; B6, descending colon; B7, skeletal muscle; B8, placenta; B9, pancreas; B10, HeLa S3; B11, foetal heart; B12, yeast tRNA; C1, frontal lobe; C2, corpus callosum; C3, thalamus; C4, left atrium; C5, duodenum; C6, rectum; C7, spleen; C8, bladder; C9, adrenal gland; C10, leukaemia K-562; C11, foetal kidney; C12, *E. coli* rRNA; D1, parietal lobe; D2, amygdala; D3, pituitary gland; D4, right atrium; D5, jejunum; D6, blank; D7, thymus; D8, uterus; D9, thyroid gland; D10, leukaemia MOLT-4; D11, foetal liver; D12, *E. coli* DNA; E1, occipital lobe; E2, caudate nucleus; E3, spinal cord; E4, left ventricle; E5, ileum; E6, blank; E7, peripheral blood leucocyte; E8, prostate; E9, salivary gland; E10, Burkitt's lymphoma Raji; E11, foetal spleen; E12, poly r(A); F1, temporal lobe; F2, hippocampus; F3, blank; F4, ventricle right; F5, ileocaecum; F6, blank; F7, lymph node; F8, testis; F9, mammary gland; F10, Burkitt's lymphoma Daudi; F11, foetal thymus; F12, human C_0t-1 DNA; G1, p.g. of cerebral cortex; G2, medulla oblongata; G3, blank; G4, inter-ventricular septum; G5, appendix; G6, blank; G7, bone marrow; G8, ovary; G9, blank; G10, colorectal adenocarcinoma SW480; G11, foetal lung; G12, human DNA 100 ng; H1, pons; H2, putamen; H3, blank; H4, apex of the heart; H5, ascending colon; H6, blank; H7, trachea; H8, blank; H9, blank; H10, lung carcinoma A549; H11, blank; H12, human DNA 500 ng.

would suggest an ability of HKE4 to alter intracellular zinc by transporting it across the membranes on which it was situated.

The ability of these cells to respond to extracellular zinc was tested by incubating them with 25 μM zinc for 15 min (Figure 6B, lower panel). This exposure to 25 μM zinc caused a small increase in the number of CHO and LacZ control cells with increased Newport Green fluorescence, whereas both LIV-1- and HKE4-transfected cells showed a 2.5–3-fold increase in this relatively short time period (Figure 6B, lower panel), consistent with the recombinant proteins causing this increase.

Furthermore, to test whether HKE4 could respond to alterations in zinc concentration, cells were incubated for a longer time period of 30 min with 25 μM of the cell-permeable zinc-specific chelator, TPEN, after initial treatment with 25 μM zinc for 30 min. The basal level of Newport Green fluorescence (Figure 6C, white bars) was similar to that observed previously, with the HKE4- and LIV-1-transfected cells showing an almost 2-fold increase in Newport Green fluorescence compared with the controls. The HKE4- and LIV-1-transfected cells responded to the increase in extracellular zinc by producing a 3- or 2-fold increase in cells with high Newport Green fluorescence respectively (Figure 6C, black bars). This increased fluorescence was reversed by the subsequent addition of cell-permeable TPEN, in both the control cells and those expressing LIV-1 (Figure 6C, hatched bars), suggesting that the source of the increased Newport Green fluorescence was extracellular. However, incubation of HKE4 expressing cells with TPEN, after zinc addition, did not completely reverse this observed increase in fluorescence. This result is consistent with some of the zinc-specific fluorescence originating from intracellular stores rather than from outside the cell and also the quenching of cytosolic zinc by TPEN increasing the transport of zinc into the cytosol by HKE4.

To test further the observed HKE4-related increase in zinc accumulation, zinc influx was measured over a short time period (Figure 6D). Both the HKE4- (filled triangles) and LIV-1- (filled squares) expressing cells had a 50 % increased mean fluorescence compared with that of the CHO (open triangles) and LacZ (open squares) control cells when incubated with 25 μM zinc, which increased further when incubated with 150 μM zinc (Figure 6D). This time- and concentration-dependent ability of HKE4-expressing cells to increase intracellular zinc was also temperature dependent as there was no evidence of cellular zinc accumulation when these experiments were repeated at 4 °C (results not shown).

Tissue distribution of HKE4 expression

It is clear from the multiple tissue expression array (Figure 7) that HKE4 is fairly ubiquitously expressed at low level with most obvious expression in the placenta (B8), liver (A9), pituitary gland (D3), pancreas (B9), salivary gland (E9), kidney (A7) and prostate (E8). Of interest is the general expression in the intestine (lanes 5A–5H and 6A–6C), which is the location of an LZT family member responsible for zinc uptake in that organ. A negative control on the array, *Escherichia coli* DNA (D12) was strongly positive for HKE4. However, this is most likely due to the presence of a family member in *E. coli* and not a cause for concern, since the other negative controls (A12, B12 and C12) were negative.

DISCUSSION

The present study provides evidence to support the inclusion of HKE4 in the LZT subfamily of ZIP zinc transporters [9,10]. We have demonstrated that HKE4 is closely related to the previously described ZIP zinc transporters, especially those of the LZT subfamily [9]. Similarities include the presence of eight TM domains with a comparable hydropathy plot to LIV-1 (Figure 2),

conserved histidine-rich repeats in three areas of the molecule (Figure 1), a ZIP consensus sequence in TM IV [6] and an LZT consensus sequence in TM V [9], both of which include the conserved histidine residues important for ZIP transporter function (Figure 3), an overall negative charge consistent with an ability to transport positively charged ions, no strong PEST site although some dibasic degradative motifs (Table 1) and an ability to increase the intracellular free zinc concentration in a time-, temperature- and concentration-dependent manner (Figure 6). All these results are consistent with HKE4 acting as a functional zinc transporter.

We have also shown that HKE4 has some unique differences from any LZT proteins investigated to date. One major discovery, with important functional implications, was the location of HKE4 on intracellular membranes including the ER, whereas most other LZT family members, namely LIV-1 [18], LZT-Hs4 [9] and other ZIP transporters, such as hZIP1 [17], hZIP2 [16], Zrt1 yeast, have been located in the plasma membrane. However, this is not completely unprecedented as one other human LZT sequence, BigM103, has been localized to intracellular structures such as lysosomes and endosomes [26].

Therefore we have shown that, when loaded with the zinc-specific fluorescent dye Newport Green, cells expressing recombinant HKE4 have increased fluorescence in a time-, temperature- and concentration-dependent manner, compatible with HKE4 increasing the Newport Green fluorescence of cells by the transport of zinc via a carrier-mediated transport process. This is the first demonstration of a human KE4 subgroup protein located on the ER membrane and with an ability to transport zinc. The direction in which HKE4 transports zinc, still undetermined, can either be into or out of the ER. For example, if HKE4 transported zinc into the ER, in the opposite direction to that predicted, this may decrease cytosolic zinc and encourage zinc influx from outside down a concentration gradient, producing the observed increase in intracellular zinc. However, our results do not suggest any delayed influx of zinc into cells when transported by HKE4 (Figure 6D) compared with that of the zinc influx transporter, LIV-1.

Our preferred explanation is the ability of HKE4 to transport zinc out of the ER (and other intracellular stores), which would be compatible with it maintaining the same membrane topology (Figure 2A) as other LZT family members that have been located to the plasma membrane [9,18]. This direction of zinc transport could produce the observed increase in intracellular-free zinc (Figure 6) in two ways. First, if the zinc in the ER was initially non-reactive to Newport Green being, e.g. protein bound, and then released as free zinc after it had been transported into the cytosol, this would produce an increase in Newport Green fluorescence. Alternatively, the same outcome could be obtained if the Newport Green indicator predominated in the cytosol, having not penetrated well into intracellular organelles. Although diacetate-conjugated indicators can accumulate in any of the membrane-enclosed structures within the cell [27], it is generally assumed for calibration purposes that the indicators are located in the cytosol [24]. If this was the case, any free zinc present in these intracellular organelles would have no fluorescence until transported into the cytosol. This conclusion is not unprecedented, as the *Arabidopsis* KE4 gene IAR1 was also suggested to reside on the ER membrane [7] and be capable of transporting metal ions out of this organelle. Interestingly, IAR1 was functionally replaced in *Arabidopsis* by mouse KE4, confirming a comparable role for KE4 sequences in plants and mammals. The human BigM103 protein, another LZT family member [9] located on intracellular vesicles, has also been shown to be capable of increasing intracellular zinc accumulation in Newport Green loaded CHO cells [26].

Further characterization of zinc transport by HKE4 into or out of intracellular stores is hampered without the availability of organelle-targeted zinc-specific indicators, such as the aequorin indicators available for calcium [28]. Overall, this result leads to the prediction that LZT members, whether located on external or internal cell membranes, can accumulate intracellular zinc in response to changes in zinc by acting as zinc transporters.

An additional LZT protein, the mouse sequence ermelin (Q8R518, 505 amino acids), has also been localized to the ER [29]. This sequence appears to be the mouse homologue of LIV-1 and as such would be expected to reside on the plasma membrane [18]. Recently, another mouse sequence (Q8C145, AK028976) with 765 amino acids has appeared in the GenBank®, which is an exact match with the previous ermelin sequence, adding a further 260 residues at the N-terminus that closely match LIV-1. This lack of N-terminal residues in ermelin may account for this potentially erroneous location and needs to be confirmed by further investigation.

HKE4, in contrast with LIV-1, failed to exhibit plasma membrane staining under high or low zinc conditions, even in non-permeabilized cells. This suggested that its location was not post-translationally controlled by zinc levels, unlike the ZIP transporter, ZRT1, from *Saccharomyces cerevisiae*, which is internalized in high zinc conditions by endocytosis [30] or the Menkes copper P type ATPase efflux pump copper transporter that resides in Golgi membranes and redistributes to the plasma membrane in the presence of increased copper [31].

Previously, HKE4 has been aligned with other ZIP transporters because of the presence of the consensus sequence for ZIP transporters in TM domain IV [6]. However, the presence of the HEXPHEXGD signature motif for LZT proteins positions KE4 sequences firmly in this LZT subfamily [9]. The presence of this unique metalloprotease motif raises the possibility that HKE4 may also have protease activity. In addition, the HKE4 sequence contains motifs recognized by proprotein convertases (Table 1), a family of degradative enzymes important in the regulation of matrix metalloproteases. In the light of this, it will be interesting to investigate any protease activity of HKE4, although the intramembrane position of this site may hamper the task.

Another difference between HKE4 and other LZT proteins is the lack of glycosylation. This may, however, be due to either the intracellular location of the protein, leading to incomplete post-translational modifications or the fact that the only potential N-linked glycan chain attachment site was situated in TM IV (Table 1). This TM domain is essential for zinc transport and therefore the attachment of a glycan chain in this position would be expected to disrupt the functionality of the protein.

In the present study, we demonstrate that HKE4 is ubiquitously expressed in the multiple tissue array (Figure 7). This result was unlike LIV-1, which was predominately expressed in hormone-regulated tissues [18]. Interestingly, HKE4 is expressed across multiple breast cancer cells but, in addition, unlike LIV-1 [32], does not correlate with oestrogen-receptor status (results not shown). It is noteworthy that HKE4 is also ubiquitously expressed in regions of the intestine (Figure 7, lanes 5A–5H and 6A–6C). Interestingly, hZIP4, a human LZT member [9], has been shown to be responsible for zinc uptake in the intestine and defects in this gene result in the zinc deficiency disease acrodermatitis enteropathica [33].

For the work reported here, we have used the sequence from accession number Q9UIQ0 (Figure 1), which agrees with that of a section of chromosome 6 (CAA20238, AL031228) and the mouse KE4 homologue (Q31125) [34]. There are other accession numbers that include variations of HKE4 especially in the C-terminal region D82060 [2,9]. The sequence we have chosen

aligns with the other LZT family members [9] and has close identity to the mouse KE4 sequence (AF100956), which suggests that the discrepancy between sequences is probably due to an unresolved compression in the cDNA sequence.

In conclusion, our observations provide further compelling evidence of the importance of LZT family members in intracellular zinc regulation. Indeed, HKE4 appears to be a regulator of intracellular re-distribution of zinc between the ER and cytosol, whereas additional family members, such as LIV-1, contribute to influx across the plasma membrane. It will be interesting to investigate further the functional co-operation of these differently located proteins. Given the increasing evidence of an important role for dysregulation of zinc and involvement of LZT family members in disease states (notably LIV-1 in breast cancer and hZIP4 in acrodermatitis enteropathica), it is essential that the importance of HKE4 expression on aberrant cell biology is now addressed.

We thank The Sanger Centre (Cambridge, U.K.) for the gift of clone 1033B10 from library RPCI5 containing the HKE4 cDNA sequence, C. Green (University of Liverpool, U.K.) for the gift of Bluescript plasmid containing LIV-1 cDNA sequence and Dr D. Llewellyn (Department of Medical Biochemistry, University of Wales College of Medicine, Cardiff, U.K.) for the gift of the anti-calreticulin antibody. We also thank the Tenovus Cancer Charity for funding this research and E. Joyce for her valued contribution to the experimental work.

REFERENCES

1 Sugawara, A., Uruno, A., Nagata, T., Taketo, M. M., Takeuchi, K. and Ito, S. (1998) Characterization of mouse retinoid X receptor (RXR)-β gene promoter: negative regulation by tumor necrosis factor (TNF)-α. Endocrinology **139**, 3030–3033
2 Ando, A., Kikuti, Y. Y., Shigenari, A., Kawata, H., Okamoto, N., Shiina, T., Chen, L., Ikemura, T., Abe, K., Kimura, M. et al. (1996) cDNA cloning of the human homologues of the mouse Ke4 and Ke6 genes at the centromeric end of the human MHC region. Genomics **35**, 600–602
3 Hanson, I. M. and Trowsdale, J. (1991) Colinearity of novel genes in the class II regions of the MHC in mouse and human. Immunogenetics **34**, 5–11
4 Janatipour, M., Naumov, Y., Ando, A., Sugimura, K., Okamoto, N., Tsuji, K., Abe, K. and Inoko, H. (1992) Search for MHC-associated genes in human: five new genes centromeric to HLA-DP with yet unknown functions. Immunogenetics **35**, 272–278
5 Nagata, T., Weiss, E. H., Abe, K., Kitagawa, K., Ando, A., Yara-Kikuti, Y., Seldin, M. F., Ozato, K., Inoko, H. and Taketo, M. (1995) Physical mapping of the retinoid X receptor B gene in mouse and human. Immunogenetics **41**, 83–90
6 Eng, B. H., Guerinot, M. L., Eide, D. and Saier, Jr, M. H. (1998) Sequence analyses and phylogenetic characterization of the ZIP family of metal ion transport proteins. J. Membr. Biol. **166**, 1–7
7 Lasswell, J., Rogg, L. E., Nelson, D. C., Rongey, C. and Bartel, B. (2000) Cloning and characterization of IAR1, a gene required for auxin conjugate sensitivity in *Arabidopsis*. Plant Cell **12**, 2395–2408
8 Taylor, K. M. (2000) LIV-1 breast cancer protein belongs to a new family of histidine-rich membrane proteins with potential to control intracellular Zn^{2+} homeostasis. IUBMB Life **49**, 249–253
9 Taylor, K. M. and Nicholson, R. I. (2003) The LZT proteins: the new LIV-1 subfamily of zinc transporters. Biochim. Biophys. Acta. Biomembranes **1611**, 16–30
10 Gaither, L. A. and Eide, D. J. (2001) Eukaryotic zinc transporters and their regulation. Biometals **14**, 251–270
11 Stathakis, D. G., Burton, D. Y., McIvor, W. E., Krishnakumar, S., Wright, T. R. and O'Donnell, J. M. (1999) The catecholamines up (Catsup) protein of *Drosophila melanogaster* functions as a negative regulator of tyrosine hydroxylase activity. Genetics **153**, 361–382
12 Vallee, B. L. and Auld, D. S. (1990) Zinc coordination, function, and structure of zinc enzymes and other proteins. Biochemistry **29**, 5647–5659
13 Vallee, B. L. and Falchuk, K. H. (1993) The biochemical basis of zinc physiology. Physiol. Rev. **73**, 79–118
14 Truong-Tran, A. Q., Carter, J., Ruffin, R. E. and Zalewski, P. D. (2001) The role of zinc in caspase activation and apoptotic cell death. Biometals **14**, 315–330
15 Koh, J. Y., Suh, S. W., Gwag, B. J., He, Y. Y., Hsu, C. Y. and Choi, D. W. (1996) The role of zinc in selective neuronal death after transient global cerebral ischemia. Science **272**, 1013–1016
16 Gaither, L. A. and Eide, D. J. (2000) Functional expression of the human hZIP2 zinc transporter. J. Biol. Chem. **275**, 5560–5564
17 Gaither, L. A. and Eide, D. J. (2001) The human ZIP1 transporter mediates zinc uptake in human K562 erythroleukemia cells. J. Biol. Chem. **276**, 22258–22264
18 Taylor, K. M., Morgan, H. E., Johnson, A., Hadley, L. J. and Nicholson, R. I. (2003) Structure–function analysis of LIV-1, the breast cancer associated protein that belongs to a new subfamily of zinc transporters. Biochem. J. **375**, 51–59
19 Thompson, J. D., Higgins, D. G. and Gibson, T. J. (1994) CLUSTAL W: improving the sensitivity of progressive multiple sequence alignment through sequence weighting, position-specific gap penalties and weight matrix choice. Nucleic Acids Res. **22**, 4673–4680
20 Taylor, K. M., Trimby, A. R. and Campbell, A. K. (1997) Mutation of recombinant complement component C9 reveals the significance of the N-terminal region for polymerisation. Immunology **91**, 20–27
21 Ma, D. and Jan, L. Y. (2002) ER transport signals and trafficking of potassium channels and receptors. Curr. Opin. Neurobiol. **12**, 287–292
22 Hauri, H. P., Appenzeller, C., Kuhn, F. and Nufer, O. (2000) Lectins and traffic in the secretory pathway. FEBS Lett. **476**, 32–37
23 Brendel, V., Bucher, P., Nourbakhsh, I., Blaisdell, B. E. and Karlin, S. (1992) Methods and algorithms for statistical analysis of protein sequences. Proc. Natl. Acad. Sci. U.S.A. **89**, 2002–2006
24 Haughland, R. P. (2001) Indicators for Ca^{2+}, Mg^{2+}, Zn^{2+} and other metal ions. In Handbook of Fluorescent Probes and Research Products, 8th edn (Gregory, J. D. and Mallery, S., eds.), Chapter 20, Molecular Probes, Eugene, OR
25 Sensi, S. L., Yin, H. Z., Carriedo, S. G., Rao, S. S. and Weiss, J. H. (1999) Preferential Zn^{2+} influx through Ca^{2+}-permeable AMPA/kainate channels triggers prolonged mitochondrial superoxide production. Proc. Natl. Acad. Sci. U.S.A. **96**, 2414–2419
26 Begum, N. A., Kobayashi, M., Moriwaki, Y., Matsumoto, M., Toyoshima, K. and Seya, T. (2002) *Mycobacterium bovis* BCG cell wall and lipopolysaccharide induce a novel gene, *BIGM103*, encoding a 7-TM protein: identification of a new protein family having Zn-transporter and Zn-metalloprotease signatures. Genomics **80**, 630–645
27 Di Virgilio, F., Steinberg, T. H. and Silverstein, S. C. (1990) Inhibition of Fura-2 sequestration and secretion with organic anion transport blockers. Cell Calcium **11**, 57–62
28 Kendall, J. M. and Badminton, M. N. (1998) Aequorea victoria bioluminescence moves into an exciting new era. Trends Biotechnol. **16**, 216–224
29 Suzuki, A. and Endo, T. (2002) Ermelin, an endoplasmic reticulum transmembrane protein, contains the novel HELP domain conserved in eukaryotes. Gene **284**, 31–40
30 Gitan, R. S., Luo, H., Rodgers, J., Broderius, M. and Eide, D. (1998) Zinc-induced inactivation of the yeast ZRT1 zinc transporter occurs through endocytosis and vacuolar degradation. J. Biol. Chem. **273**, 28617–28624
31 Petris, M. J., Mercer, J. F., Culvenor, J. G., Lockhart, P., Gleeson, P. A. and Camakaris, J. (1996) Ligand-regulated transport of the Menkes copper P-type ATPase efflux pump from the Golgi apparatus to the plasma membrane: a novel mechanism of regulated trafficking. EMBO J. **15**, 6084–6095
32 Manning, D. L., McClelland, R. A., Knowlden, J. M., Bryant, S., Gee, J. M., Green, C. D., Robertson, J. F., Blamey, R. W., Sutherland, R. L., Ormandy, C. J. et al. (1995) Differential expression of oestrogen regulated genes in breast cancer. Acta Oncol. **34**, 641–646
33 Wang, K., Zhou, B., Kuo, Y. M., Zemansky, J. and Gitschier, J. (2002) A novel member of a zinc transporter family is defective in acrodermatitis enteropathica. Am. J. Hum. Genet. **71**, 66–73
34 Strausberg, R. L., Feingold, E. A., Grouse, L. H., Derge, J. G., Klausner, R. D., Collins, F. S., Wagner, L., Shenmen, C. M., Schuler, G. D., Altschul, S. F. et al. (Mammalian Gene Collection Program Team) (2002) Generation and initial analysis of more than 15000 full-length human and mouse cDNA sequences. Proc. Natl. Acad. Sci. U.S.A. **99**, 16899–16903
35 Hofmann, K. and Stoffel, W. (1993) TMbase – a database of membrane spanning proteins segments. Biol. Chem. Hoppe-Seyler **347**, 166–172
36 Molloy, S. S., Anderson, E. D., Jean, F. and Thomas, G. (1999) Bi-cycling the furin pathway: from TGN localization to pathogen activation and embryogenesis. Trends Cell Biol. **9**, 28–35
37 Seidah, N. G. and Chretien, M. (1999) Proprotein and prohormone convertases: a family of subtilases generating diverse bioactive polypeptides. Brain Res. **848**, 45–62

Received 5 August 2003/22 September 2003; accepted 3 October 2003
Published as BJ Immediate Publication 3 October 2003, DOI 10.1042/BJ20031183